Hindawi
Geofluids
Volume 2020, Article ID 8894030, 18 pages
https://doi.org/10.1155/2020/8894030

Research Article

Evaluation of Hydrocarbon Generation Using Structural and Thermal Modeling in the Thrust Belt of Kuqa Foreland Basin, NW China

Chengfu Lyu,[1,2] **Xixin Wang**,[3] **Xuesong Lu**,[4,5] **Qianshan Zhou**,[1,2] **Ying Zhang**,[1] **Zhaotong Sun**,[1] **Liming Xiao**,[3] **and Xin Liu**[3]

[1]*Northwest Institute of Eco-Environment and Resources, Chinese Academy of Sciences, Lanzhou 730000, China*
[2]*Key Laboratory of Petroleum Resources, Gansu Province, Lanzhou 730000, China*
[3]*School of Geosciences, Yangtze University, Wuhan 430100, China*
[4]*Research Institute of Petroleum Exploration& Development, Petrochina, Beijing 100083, China*
[5]*Key Laboratory of Basin Structure and Hydrocarbon Accumulation, CNPC, Beijing 100083, China*

Correspondence should be addressed to Xixin Wang; wxxdyx_33@163.com

Received 17 August 2020; Revised 9 November 2020; Accepted 27 November 2020; Published 18 December 2020

Academic Editor: Shiyuan Zhan

The Kuqa Basin is a typical foreland basin in northwest China, characterized by compressive foreland fold-and-thrust belts and a regionally distributed huge salt layer. A large number of overthrust faults, fault-related folds, and salt-related structures are formed on the thrust belt due to strong compression and structural deformation, causing difficulty in simulation of the basin. In this study, modeling of the thermal history of the complicated compressional structural profiles in the Kuqa foreland basin was successfully conducted based on the advanced "Block" function introduced by the IES PetroMod software and the latest geological interpretation results. In contrast to methods used in previous studies, our method comprehensively evaluates the influence of overthrusting, a large thick salt layer with low thermal conductivity, fast deposition, or denudation on the thermal evolution history. The results demonstrate that the hydrocarbon generation center of the Kuqa foreland basin is in the deep layers of the Kelasu thrust belt and not in the Baicheng Sag center, which is buried the deepest. A surprising result was drawn about the center of hydrocarbon generation in the Kuqa foreland basin, which, although not the deepest in Baicheng Sag, is the deepest part of the Kelasu thrust Belt. In terms of the maturity of the source rock, there are obvious temporal and spatial differences between the different structural belts in the Kuqa foreland basin, such as the early maturation of source rocks and the curbing of uplift and hydrocarbon generation in the piedmont zone. In the Kelasu thrust belt, the source rock made an early development into the low mature-mature stage and subsequently rapidly grew into a high-over mature stage. In contrast, the source rock was immature at an early stage and subsequently grew into a low mature-mature stage in the Baicheng Sag–South slope belt. The time sequence of the thermal evolution of source rocks and structural trap formation and their matching determines the different accumulation processes and oil and gas compositions in the different structural belts of the Kuqa foreland basin. The matching of the multistage tectonic activity and hydrocarbon generation determines the characteristics of the multistage oil and gas accumulation, with the late accumulation being dominant. The effective stacking of the gas generation center, subsalt structural traps, reservoir facies of fine quality, and huge, thick salt caprocks creates uniquely favorable geological conditions for gas enrichment in the Kelasu foreland thrust belt.

1. Introduction

The Kuqa foreland basin, located between the Tianshan Mountains to the north and the north Tarim uplift to the south, is a Meso-Cenozoic foreland basin, which is a vital natural gas exploration and development base in China. There are two sets of thick salt layers each in the west and east of the basin. The Kuqa foreland basin currently has the

highest reserves of discovered natural gas and the largest single gas reservoir size; the level of oil and gas exploration and research is also the highest. The discovery of gas fields such as Kela-2, Dina-2, and Yaha in 1998 has led to the discovery of a number of gas fields (reservoirs) such as Dabei, Keshen-2, Keshen-5, and Keshen-8 in deep layers with depths of 6–8 km in the Kelasu tectonic belt. The geological setting of the above discoveries is mostly distributed in the foreland thrust belt. The width of the basin is 20–60 km, and the area is approximately 28500 km^2 (Figure 1). The basin is characterized by compressive foreland fold-thrust belts [1–6]. The geometry of the basin is an asymmetric wedge where the flank adjacent to the Tianshan orogenic belt has a greater sediment thickness than that towards the Tarim craton. The strong compressive structural deformation has formed many fault-related folds and salt-related structures in the thrust belt, causing challenges in the process of modeling of the basin. The reasons are as follows: (1) constructing and computing the complicated thrust-faulted 2D geological model in most basin modeling software, including IES PetroMod, TemisFlow, BasinMod, and Trinity, is usually challenging; (2) a unique aspect of the thermal history of thrust belts is that the hanging wall and footwall undergo different time-temperature paths [7–9]. During thrusting, the hanging wall is uplifted and undergoes rapid cooling, while the footwall undergoes initial warming due to tectonic burial [9]. (3) Owing to the thrust faulting and salt movement, the burial history near the fault changes unconventionally and abruptly, which is difficult to consider in 1D basin modeling.

Due to the large burial depth of the Triassic–Jurassic source rocks with fewer experimental data, the study of source rock maturity and hydrocarbon generation evolution mainly relies on basin modeling. Previous studies mainly used simple 1D single-well simulation and basin modeling based on thickness maps without considering overthrust faulting and salt deformation [10–12]. Additionally, a number of previous studies have been carried out on the history of hydrocarbon charge of this area. Li et al. (1999) concluded that the oil and gas accumulations formed during the late Neogene, and Lü and Jin (2000) proposed that the hydrocarbons accumulated during the late Paleogene to Quaternary based on an integrated analysis of the trap formation and timing of petroleum generation. Liu et al. (2016) analyzed the timing of the oil charge in the Yangtake area. Other studies have investigated the charge history of the entire Kuqa foreland basin [10, 13, 14] that may be relevant for the Yangtake fold belt. However, a more detailed quantitative study of the distribution and phase state of the oil and gas fields discovered so far does not match the required source rock maturity distribution. In order to better explain the current exploration status (oil and gas distribution) and thus guide the direction of oil and gas exploration, it is necessary to use new basin modeling technology to relearn the hydrocarbon generation evolution of source rocks in the Kuqa foreland basin.

In this study, the advanced "TecLink" concept provided by the PetroMod® petroleum system modeling software was used, which efficiently solves the difficult problem of basin modeling in complicated thrust belts. Moreover, the source rock maturation and hydrocarbon generation histories of the Kuqa foreland basin were investigated to rediscover the thermal evolution of source rocks and maturity distribution and best explain the observed distribution of the discovered oil and gas. The modeling considers the effect of thrust faulting, salt layer, rapid deposition, and denudation on the thermal evolution and source rock maturation. The results show that the hydrocarbon generation center of the Kuqa foreland basin is not in the Baicheng Sag center with the deepest buried depth but in the deep layers of the Kelasu thrust belt. The results differ from those of previous studies [10–12] and perfectly match the discovered oil and gas distribution.

2. Geological Setting

2.1. Structural Characteristics. The Kuqa foreland basin, located on the northern margin of the Tarim block, is a transitional site between the South Tianshan and Tarim blocks. The formation and evolution of the Kuqa foreland fold belt are related to the multiphase reactivated and uplifted Tianshan orogenic belt during the Meso-Cenozoic [3]. Under compressive tectonic loading and gravitational loading, the Kuqa depression became an intracontinental foreland basin. The cross-section of the basin is asymmetric, and its depocenter lies close to the Tianshan orogenic belt. The sediment thickness thinned towards the Tarim craton.

The tectonic styles are dominated by thrust folds developed during the Cenozoic. They show vertical layering and zoning oriented in a north–south direction. A series of south-vergent thrust and fold beds in the Kuqa foreland basin oriented from north to south can be divided into six subunits (Figure 1): (1) northern monocline belt, (2) Kelasu-Yiqikelike structural belts, (3) Baicheng-Yangxia Sags, (4) Qiulitage structural belts, (5) southern frontal uplift belt, and (6) Wushi Sag. The basin modeling and thermal history discussed in this paper are mainly distributed in the middle segment of the Kuqa foreland thrust belt, involving the following: northern monocline belt, Kelasu structural belt, Baicheng Sag, and southern frontal uplift. Vertically influenced by the Paleogene and Neogene gypsum-salt beds, Li et al. [15] suggested that the tectonic deformation of the Qiulitag fold structure was thin-skinned, and the deformation of the subsalt strata mainly accumulated in the hinterland. The deformation above the salt strata is mainly fault-propagation folds and detachment folds, while the structural style comprises a wedge of southerly vergent thrust sheets [16].

2.2. Stratigraphy and Source Rock. Mesozoic and Cenozoic strata are fully developed in the Kuqa Foreland basin. From the Triassic to Cenozoic, the strata can be divided into 17 sets, with a depth of approximately 100 km (Figure 2). The two Triassic and Jurassic sequences can be subdivided into five sequence sets from top to bottom, which are the main source rocks; these include the upper Triassic Huangshanjie set (T_3h) and Taliqike set (T_3t), 1ower Jurassic Yangxia set (J_1y), middle Jurassic Kezilenuer set (J_2kz), and the bottom of the Qiakemake set (J_2q) [12, 17, 18]. Among them, T_3h and J_2q are mainly lacustrine mudstones, while the other

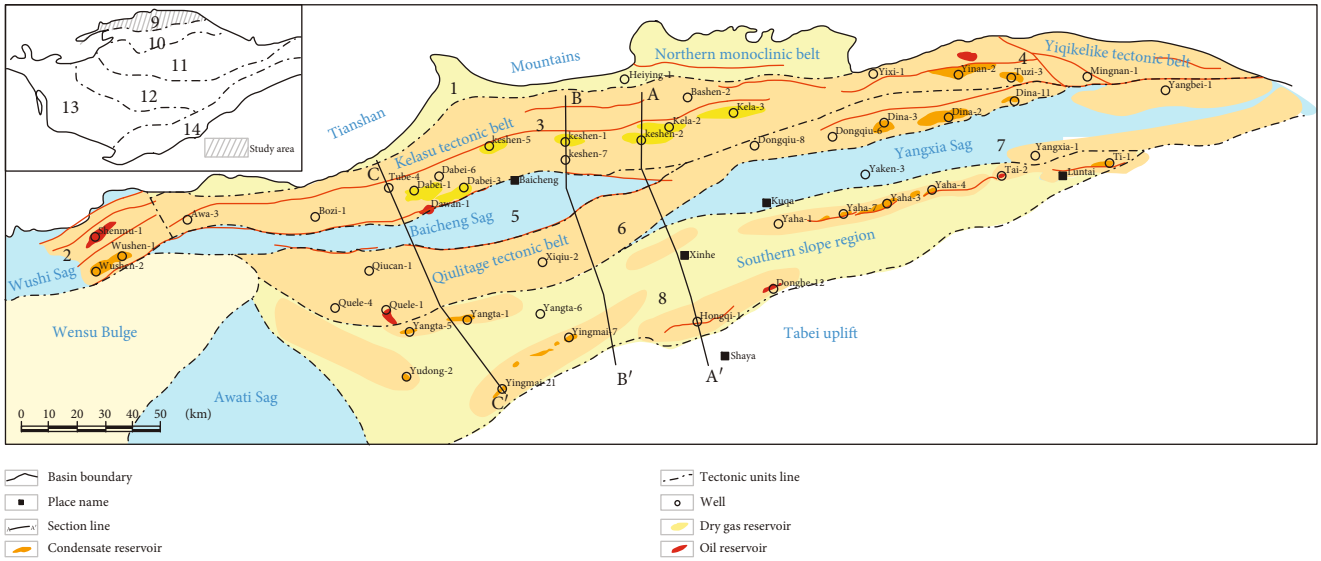

Figure 1: Sketch map of the Kuqa foreland basin (modified from Lu et al., 2018): (1) North monocline zone; (2). Wushi Sag; (3) Kelasu structural belt; (4) Yiqikelike structural belt; (5) Baicheng Sag; (6) Qiulitage structural belt; (7) Yangxia Sag; (8) South slope belt; (9) Kuqa depression; (10) Tabei uplift; (11) Northern depression; (12) the central uplift; (13) Southwest depression; (14) Tadong uplift.

three sets are coal-bearing measures. Generally, coal measure source rocks are more extensively developed than the lacustrine mudstones.

In the Kuqa foreland basin, three important regional reservoir-seal combinations are developed [19] (Figure 2): (1) thin sandstone at the bottom of N_1j, E-K sandstone–N_1j evaporate rock and mudstone; (2) $E_{1\text{-}2}$km basal conglomerate, K_1bs sandstone–$E_{1\text{-}2}$km giant and thick evaporate rock; and (3) J_1a sandstone–J_1y coal measures. Good reservoir-seal assemblages control the occurrence of the oil and gas reservoirs. The large oil and gas fields discovered (Dina-2, Kela-2, and Yinan-2) are related to the three reservoir-seal assemblages separately.

2.3. Oil and Gas Discoveries. Since 1993, giant gas fields, such as Kela-2, Dina-2, and Yaha, have been discovered, and a total of 42 oil and gas reservoirs have been discovered in the Kuqa petroleum system, with over 1000 billion cubic meters (bcm) and over 100 million tons of proven gas and oil reserves, respectively [20–23]. These include four gas fields, eight gas condensate fields, and three oil fields (Figure 1). These discoveries make the Tarim basin one of the top three basins with significant gas resources in onshore China, while the others are the Ordos and Sichuan basins. The distribution characteristics of oil and gas in the Kuqa petroleum system are as follows: (1) this system is mainly rich in gas, with a small amount of oil, and the proven gas reserve is nine times that of the oil reserve; (2) the gas reserve is mainly located in the north thrust belt that contains 91% of the total gas reserve; and (3) the hydrocarbon phase state is diverse. The north is rich in gas, especially dry gas, such as the Kela-2, Dabei, and Keshen-2 gas fields. In contrast, the south relatively lacks gas and gas condensate reservoirs with a low-middle gas-oil ratio. Many studies have focused on the Dawanqi oil field [18, 24], Kela-2 gas field [10, 25], and Dabei gas field [26]. The differences in the oil and gas phases are mainly affected by the maturity and accumulation processes, which are closely related to each other [27, 28].

3. Basin Modeling: Conceptual Model and Input

Basin modeling is a powerful tool for the evaluation of temperature and maturity evolution, petroleum generation, and migration from potential source rocks in sedimentary basins [29–33]. The study was conducted using the *PetroMod v11* software package developed by Integrated Exploration Systems (IES), Germany. It is based on the description of physical and chemical phenomena that control the formation of commercial accumulations within sedimentary basins: deposition, compaction, heat transfer, hydrocarbon generation, and multiphase fluid flow [32, 34].

A 3D petroleum system model of the Kuqa Basin was constructed using the PetroMod V11 software. As part of this study, data from 7 deep exploration wells within the study area were used to set up a 1D model for calibration. Furthermore, three sections running N–S, as shown in Figure 1, were selected to set up a 2D model by using the advanced "PetroMod TecLink" technique. Modeling the complex tectonic environments such as thrust belts requires the sections to be restored structurally and kinematically. In this study, several balanced paleo-sections were used to model the temperature and maturity history of the section.

3.1. Construction of the Geological Models. Heat flow models can be calibrated with the measured temperatures from wells and thermal maturity parameters, such as the vitrinite reflectance, biomarkers, and fission-track annealing data [34]. However, the most commonly used parameter is vitrinite reflectance as it is widely available in most sediment types, covers typical oil and gas maturity ranges, and is easy and inexpensive to measure. In this study, the vitrinite reflectance was based on the standard used to microscopically determine

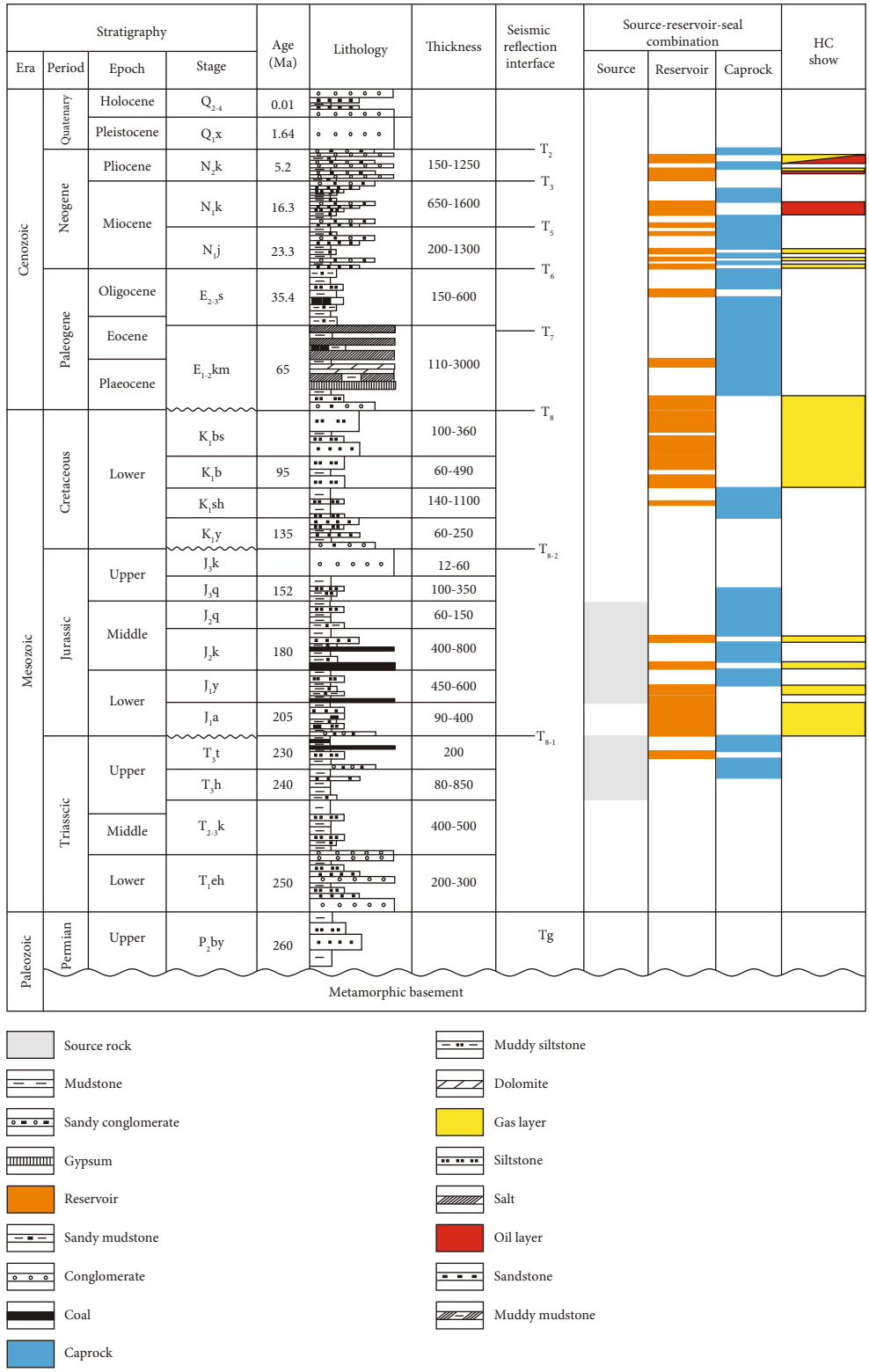

Figure 2: The integrated histogram of the Kuqa petroleum system.

the vitrinite reflectance in the sediments of China (SY/T 5124-2012). For the 1D modeling, 7 wells with completely measured temperature or vitrinite reflectance (Ro%) data such as Yinan-2, Dawan-1, Kela-2, Yingmai-7, Yangta-101, YangXia-1, and Dongqiu-5 were used. Furthermore, two virtual wells, YX and BC, located at the center of Yangxia Sag and Baicheng Sag separately, were modeled to analyze the burial and thermal history of the two sag centers. For the simulations, input models were created from the stratigraphic data consisting of a continuous sequence of events

Table 1: Lithology, thermal conductivity, and boundary condition used in the basin modeling.

Strata	Geological time (Ma)	Main lithology	Main sedimentary faces	Thermal conductivity (W/m/K)	Average paleo surface temperature (°C)	Average paleo water depth (m)	Average paleo heat flow (mW/m^2)
Q	1.6	Conglomerate	Piedmont-alluvial fan	2.93	15	0	45.00
N_2k	5.2	Pebbly sandstone	Fluvial	2.93	15	0	47.25
$N_{1\text{-}2}k$	16.3	Sandstone, silty sandstone	Fluvial-floodplain	2.78	14	2	48.00
N_1j	25.3	Silty mudstone, mudstone	Dry lake	2.78	19	8	49.00
$E_{2\text{-}3}s$	35.4	Silty mudstone	Shallow lake	2.05	21.1	6	49.40
$E_{1\text{-}2}km$	65	Gypsum-salt, gypsum mudstone	Salt lake	3.87	21.99	10	50.00
K	135	Fine-grained sandstone, siltstone	Braided fluvial-delta	2.97	24.61	5	50.40
J	205	Coal shale	Shallow lake-swamp	1.8	18.82	15	51.00
T	245	Mudstone with coal line	Semideep lake-deep lake	1.98	20.27	30	51.50

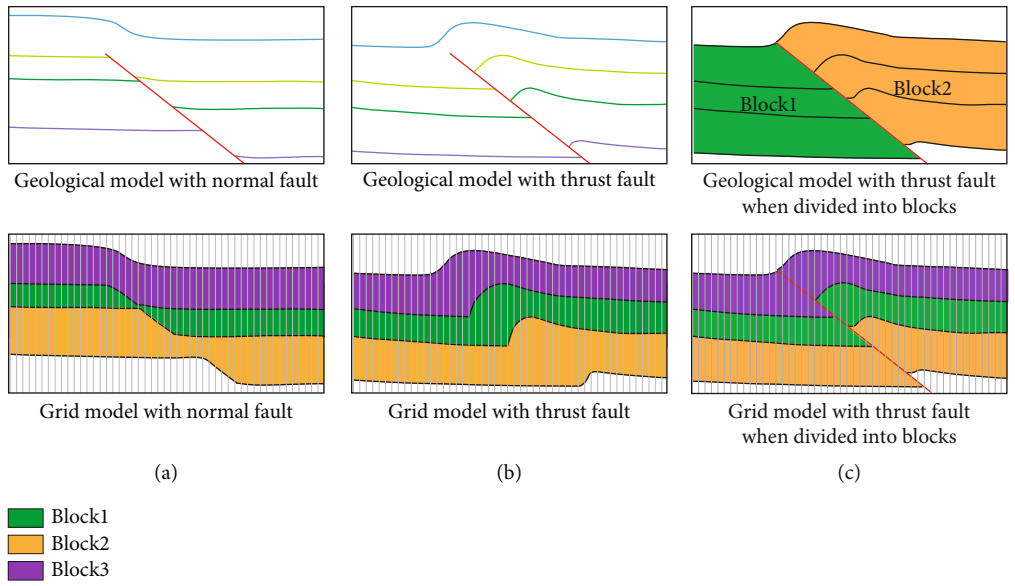

Figure 3: Comparison of geological models and grid models with normal or thrust fault.

(Table 1). Strata thicknesses and lithologies were obtained from well reports. The petrophysical properties of the various lithologies were provided by the modeling package (Table 1). The basement heat flow data were set according to previous research results [35–38] and single well calibration. The result of the thermal history restoration shows that the Kuqa foreland basin was always at a low heat flow state since the Triassic. It relatively hot in the Mesozoic (50–55 mW/m^2), while the heat flow decreased slowly but continuously since the Cenozoic and decreased rapidly since 2 Ma, eventually reaching today's heat flow of 40–46 mW/m^2 (Table 1).

For the 2D modeling, several sections running N–S were selected, while just one section through the Keshen-2 well was selected as an example to show the specific modeling process. The interpreted strata lines from the seismic data were input into the PetroMod® software package, where the conceptual models were created and transferred into finite element grids consisting of nine geological events along the section line (Table 1).

3.2. "Block" Model for Complex over Thrusted Geological Profiles. In most basin modeling software, including Temis-Flow, BasinMod, and Trinity, 2D basin modeling is realized by layer-based gridding from the geological model, requiring the same layer to occur only once along one vertical grid line. For a simple geological profile with normal faults, the layer line after gridding can be treated as extending along the fault plane (Figure 3(a)), and the conceptual model after gridding is not significantly different from the original geological model in the details near the normal fault. However, some tectonic settings are complex. Moreover, if overthrusting occurs, a horizon/layer may be defined by multiple z-values

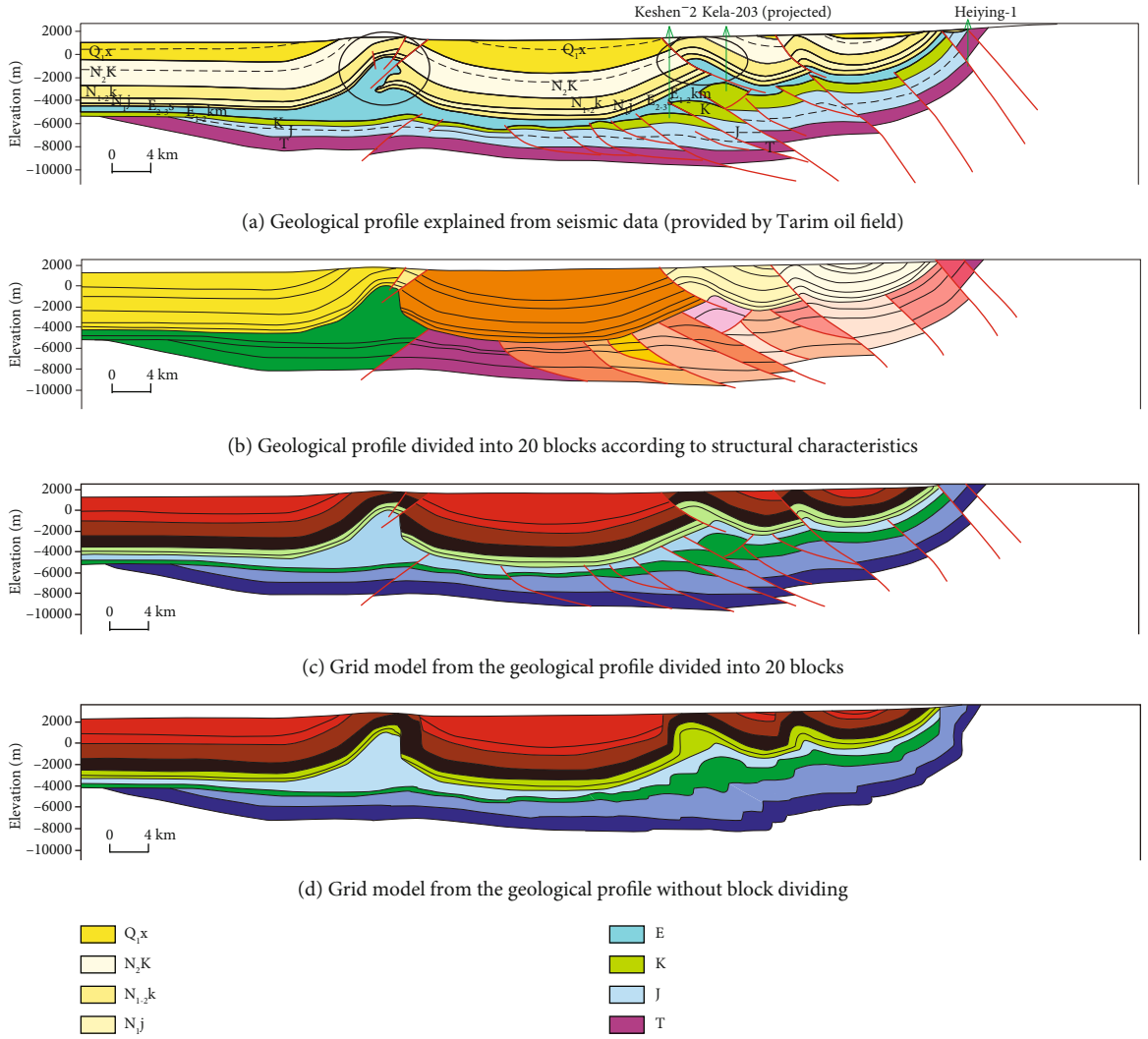

(a) Geological profile explained from seismic data (provided by Tarim oil field)

(b) Geological profile divided into 20 blocks according to structural characteristics

(c) Grid model from the geological profile divided into 20 blocks

(d) Grid model from the geological profile without block dividing

Figure 4: Geological section through the Keshen-2 well and the geological model with blocks.

on one vertical grid line. Conventional methods cannot deal with such complex situations; this change is ignored when gridding, so the conceptual model after gridding will have a large difference compared to the original model in the detailed structural shape near the thrust fault (Figure 3(b)).

With the PetroMod TecLink concept, PetroMod's finite element simulator is able to handle such multiple z-values on one vertical grid line [34, 39]. A block is defined by a characteristic layer stack with no multiple z-values within its boundaries. Each block is then treated as a "single basin model," with suitable and varying coupling conditions between the block boundaries. The 2D sections can be split into several blocks. The geological model with the thrust fault shown in Figure 3(c) can be divided into two blocks by the fault boundaries. Subsequently, the conceptual model after gridding can reflect the original structural details. By comparison, the "block" function has obvious advantages in the modeling of foreland thrusting complex settings. Each paleo-section is split into several blocks specified by its boundaries and a characteristic layer stack. The number of blocks can vary during the paleo steps, as the breaking of a so-called superblock into separate pieces leads to the development of complex block substructures from a homogeneous initial model. A hierarchy of block heritages must be specified as the model input. The splitting of a superblock into subblocks must also be taken into account when considering the shift of the fundamental layer values based on their new locations.

In the geological section through the Keshen-2 well (Figure 4(a)), considering the $E_{1\text{-}2}$km plastic salt layer as a boundary, the suprasalt and subsalt strata have totally different structural deformation characteristics [15, 40]. Apart from the shallow area in the northern monocline region, the subsalt thrust faults basically disappeared in the salt layer. According to the actual profile geological characteristics, the scheme for block model establishment is as follows: the suprasalt and subsalt strata are divided into two "block" systems; the subsalt thrust fault can be extended into the $E_{1\text{-}2}$km salt layer top, and each thrust fault block can then be classified as a "block," considering the thrust fault as a boundary. Using this "block" function, the profile was divided into 20 separate "blocks" (each color in Figure 4(b) represents a

Table 2: The vitrinite reflectance (Ro, %) of the source rock in outcrops and wells in the Kuqa Basin.

Strata	Awate River outcrop	Kapushaliang River outcrop	Kelasu River outcrop	Kuqa River outcrop	Tugeerming outcrop	Yinan-2 well	Yangxia-1 well
J	1.83	0.79~1.35		0.60~0.88	0.58~0.61	1.03~1.35	0.95~1.10
T		1.74~1.87	0.62~0.76 1.43	1.13~1.15 0.56~0.75	0.67	1.32~1.45	

"block"). To achieve better simulation results, simplification processing was performed in some very complex local areas. For example, in the circle area of Figure 4(a), the salt pierced through the rock layer, and such a complex structure cannot be dealt with, so the block model was simplified relative to the actual profile. The grid model from the block model is shown in Figure 4(c). It can be seen that this can provide a good indication of the structural complexity of the actual profile, even in some detailed structural features. This is another conventional basin modeling software that cannot be achieved, fully reflecting the advancement of the "block" technology.

It is challenging to accurately recover the geological profile history because of the complex structural shapes in the foreland thrust belt, consequently having to rely on conventional backstripping technology. The balanced profiles of the geological history were input into the software, and a block model was set up in the same way. In the entire process of continuous evolution modeling of the geological section, the influence of the overthrusting process, salt plastic flow, rapid deposition or erosion on heat flow, and source rock maturation was well simulated. This is thus more convenient and intuitive than multiple single-well simulations.

Heat flow analysis is based on a detailed balance of thermal energy that is transported through heat flow through the sedimentary basins. The main direction of heat flow in sedimentary basins is vertically upward. It is thus possible to demonstrate the basic effects using crude 1D model. Steady-state heat flow constitutes the simplest heat flow model. The assumption of the steady-state heat flow is based on the fact that all time-dependent terms such as transient or convection effects are neglected, and the same formation temperature does not change with time. This has been observed in both experimental studies and numerical simulations (Morris, 1968; [25]). Therefore, the temperatures at all layer boundaries can be calculated from the surface temperature down to the base of the section [34]. However, the heat flow from the base upward does not remain constant with change in time, and any change in the thermal boundary condition, geometry, properties, or temperatures yields a nonsteady or transient state. The system gradually returns to a new flow equilibrium when the new conditions stop changing. The transition time generally depends on the ratio of the transported heat to the inner thermal energy, which is controlled by the size of the system and the ratio of the heat capacity and the thermal conductivity.

The transient effect is important during deposition and erosion and during the rapid change of the thermal boundary conditions or basal heat flow. Deposition results in deeper burial and higher temperatures of underlying sediments, causing the actual sediment temperatures to be lower than that of the steady-state flow [34]. Therefore, the transient heat flow method should be used to simulate the formation temperature when considering the actual geological processes.

In this study, the transient heat flow method was used in the thermal modeling. This method has the following advantages: (1) compared with the geothermal gradient method, this method can consider the effect of different lithologies on temperature, especially those of special lithology like gypsum and salt rock [38, 41]; (2) compared with the steady-state heat flow method, the transient heat flow method can consider the transient effect of rapid sedimentation or erosion [8]; (3) combined with the "block" technique, it can consider the impact of some special geological processes such as overthrust [7] and salt plastic flow on the thermal evolution of source rock.

4. Modeling Results

4.1. Source Rock Maturity Data. As the main source rock is at great depth in the Kuqa foreland basin, the wells currently drilled in Jurassic and Triassic source rocks are mainly distributed in the north monocline, along with shallow buried areas in the Yiqikelike tectonic belt and southern slope belt. Additionally, Jurassic and Triassic source rocks also occurred in the outcrops in the northern part of the basin boundary. However, source rocks have not yet been drilled in the abdomen due to the very large depth, and the maturity of the source rock is still unknown.

The vitrinite reflectance (Ro) is an important parameter that provides information on the organic matter quality of the source rocks (Peters and Cassa, 1994; [42] Hunt, 1996 [43]). The Ro data of the source rock in the major outcrops and drilled wells are presented in Table 2 (the location of the outcrops and sample wells is shown in Figure 5). The high striking amounts of vitrinite content usually provide valuable information on the maturation of source rock examined under plane-polarized reflected light (Hakimi et al., 2020 [44]). The Ro values of the analyzed samples ranged from 0.56 to 1.87% (Table 2). This indicates that the thermal maturity of the source rock in the studied wells ranged between mature and late-mature oil windows. Additionally, the Ro values of the study wells show a direct relationship between the burial depth and degree of maturity. Furthermore, the source rock maturity in the Kuqa foreland basin has the following characteristics: (1) the source rock Ro in the northern outcrops is all greater than 0.5%, indicating that they have had varying degrees of burial and were then raised up to the surface. (2) The source rock Ro has large differences in various outcrops, showing an overall variation with high Ro in the west and south and low Ro in the east and north. (3)

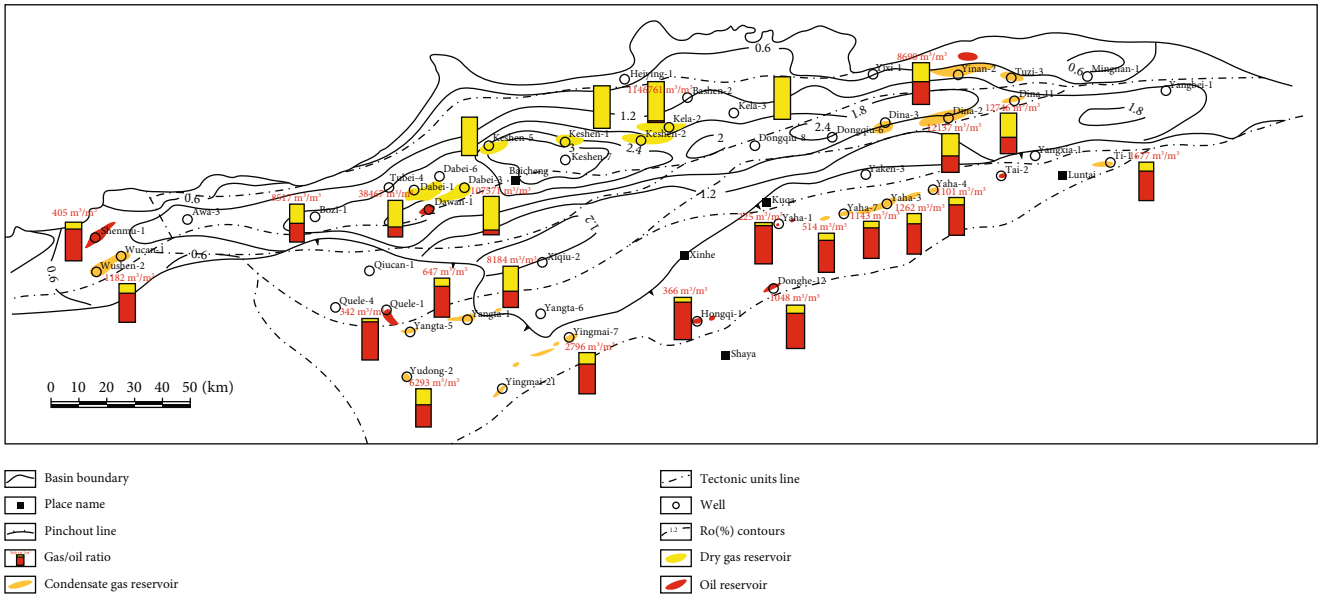

Figure 5: Congruency map of the oil and gas phase state and the source rock Ro in the Kuqa foreland basin.

In some outcrops and wells, the source rock Ro changes in a complex manner, showing that Ro does not monotonically increase or decrease but abnormally do so from the newer to older strata. For example, in the Kuqa River outcrop, there were two groups of Ro (1.13–1.15%, 0.63–0.75%) in T_3t, while Ro was 0.63–0.75% in the underlying T_3h. On the one hand, this anomaly is related to the regional complex over thrusting; conversely, it is caused by an abnormal thermal event for the spontaneous combustion of coal measures. (4) In a series of wells drilled around Yangxia Sag, such as the Yang-1, Yinan-2, Yishen-1, and Yixi-1 wells, the middle-lower Jurassic source rocks have a similar maturity with an Ro of 0.9–1.1%, even with significant differences in their current burial depth. The source rocks in the same stratigraphic positions with different depths have similar Ro values, reflecting that the maturation of the organic matter was stereotyped before the overthrusting.

4.2. Maturity Evolution and Hydrocarbon Generation

4.2.1. Single Well 1D Modeling Results. To analyze the hydrocarbon generation history of the Jurassic and Triassic source rocks in the Kuqa foreland basin, two typical wells were selected for further analysis. Yinan-2 well in the east and the artificial BC well in the center of Baicheng Sag were chosen as examples.

The burial and thermal history of the Yinan-2 well is shown in Figure 6. In the Yinan-2 well, the Ro values of the Jurassic and Triassic source rocks were less than 0.7% even at the end of Cretaceous sedimentation and had not yet transitioned into hydrocarbon generation. Subsequently, the Cretaceous uplift and erosion occurred, and the hydrocarbon generation remained stagnant for some time, until the Neogene rapid subsidence. The source rock Ro then increased rapidly and reached its maximum value at the end of the Kuqa formation sedimentation. The Ro of Jurassic source rock reached 1.0–1.3% and that of Triassic source rock reached 1.3–1.6%, indicating the wet gas generation stage. The tectonic uplift and erosion took place at the end of the Kuqa period with a large erosion thickness, thereby halting the hydrocarbon generation. Even with a small amount of Quaternary deposits, the source rock Ro did not change. As seen from the thermal evolution history of the Yinan-2 well (Figure 6), the source rock maturation and hydrocarbon generation mainly occurred in the Neogene, wherein the Ro reached its maximum value at the end of the Kuqa period. This provided the oil and gas resource base for the late large-scale hydrocarbon accumulation.

The burial and thermal history of the BC well is shown in Figure 7. The J-T source rock in the Baicheng Sag center was superficially buried before the Paleogene and did not yet reach the mature stage. Conversely, it was rapidly buried since the Neogene, especially within the huge thickness of the N2k formation, and the source rock Ro increased rapidly. At the end of the Kuqa stage, the depth of the source rock reached 6000 m, and the Ro reached a maximum of 0.9–1.1%; however, this was still at the early stage of oil generation. Although the Quaternary sediment thickness was large, the heat flow and geothermal gradient reduced, thus increasing the source rock Ro only slightly.

From the burial and thermal evolution history of many single wells, it can be seen that the maximum Ro of the J-T source rocks in the Kuqa foreland basin occurred at the end of the Kuqa stage, owing to the rapid subsidence since the Neogene. Additionally, the main hydrocarbon generation occurred rapidly from 5 Ma, which determines the mass hydrocarbon generation and expulsion, and the accumulation time was late, mainly starting from 5 Ma.

4.2.2. 2D Modeling Results of the Geological Profile. The tectonic and thermal evolution history of the geological section running N–S through the Keshen-2 well is shown in Figure 8. In the Paleogene to N_2k period, the deposition and subsidence center were close to the Tianshan Piedmont belt, and

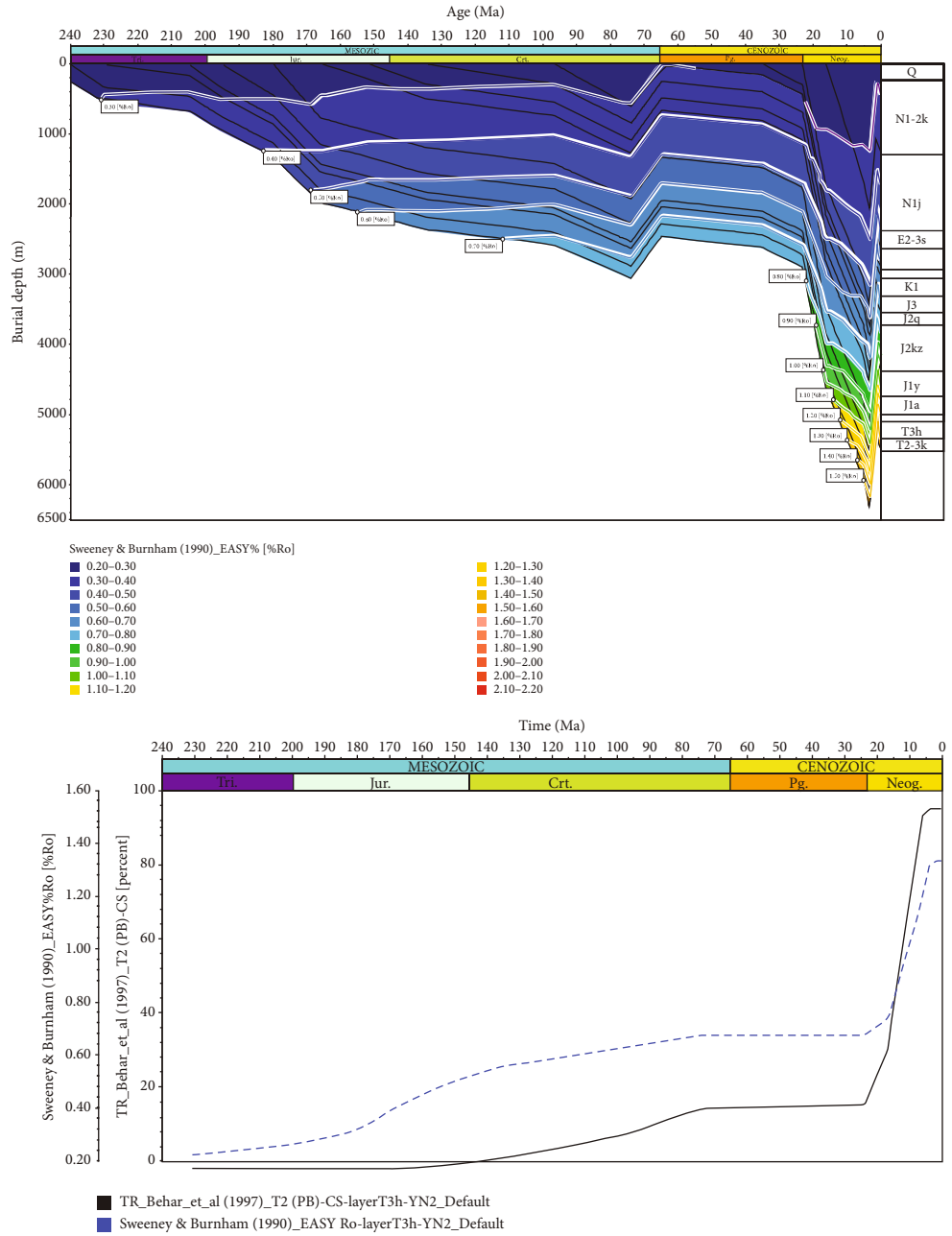

Figure 6: The burial history and Ro evolution of the Yinan-2 well.

the Jurassic and Triassic source rocks in the Piedmont belt had already entered the mature-high mature generation stage. Moreover, to the south slope, the strata thickness decreased, and the Ro was still low in the low mature–immature generation stage. In the $N_{1\text{-}2}k$ period, the overthrust began in the piedmont and extended to the basin center. In the Quaternary, large-scale thrust-imbricated structures developed, and the Keshen structural belt and the north side of Baicheng Sag became the subsidence center; here, the source rock Ro reached its maximum and entered the high-over mature dry gas generation stage. From the viewpoint of Ro evolution, there are obvious differences in different structural belts. (1) In the Piedmont belt, the maximum source rock Ro was attained before the massive thrust faulting at the end of the N_2k period. The Triassic source rock entered the mature stage and generated early oil; this was followed by intense tectonic uplift and erosion that halted the hydrocarbon generation. (2) The north side of the Kelasu structural belt generated early oil at the end of the N_2k period as the source rock Ro was already high, i.e., in the mature-high mature generation stage. The overthrust and stack effect since the $N_{1\text{-}2}k$ period further increased the depth, thereby further increasing the Ro to a maximum of 3.0%. A large quantity of dry gas was generated in the late stage and has become the largest gas generation center today. (3) On the south side of the Kelasu structural belt and to the north of Baicheng Sag, the source rock was still in a low mature stage at the end of the N_2k period. However, the overthrust and

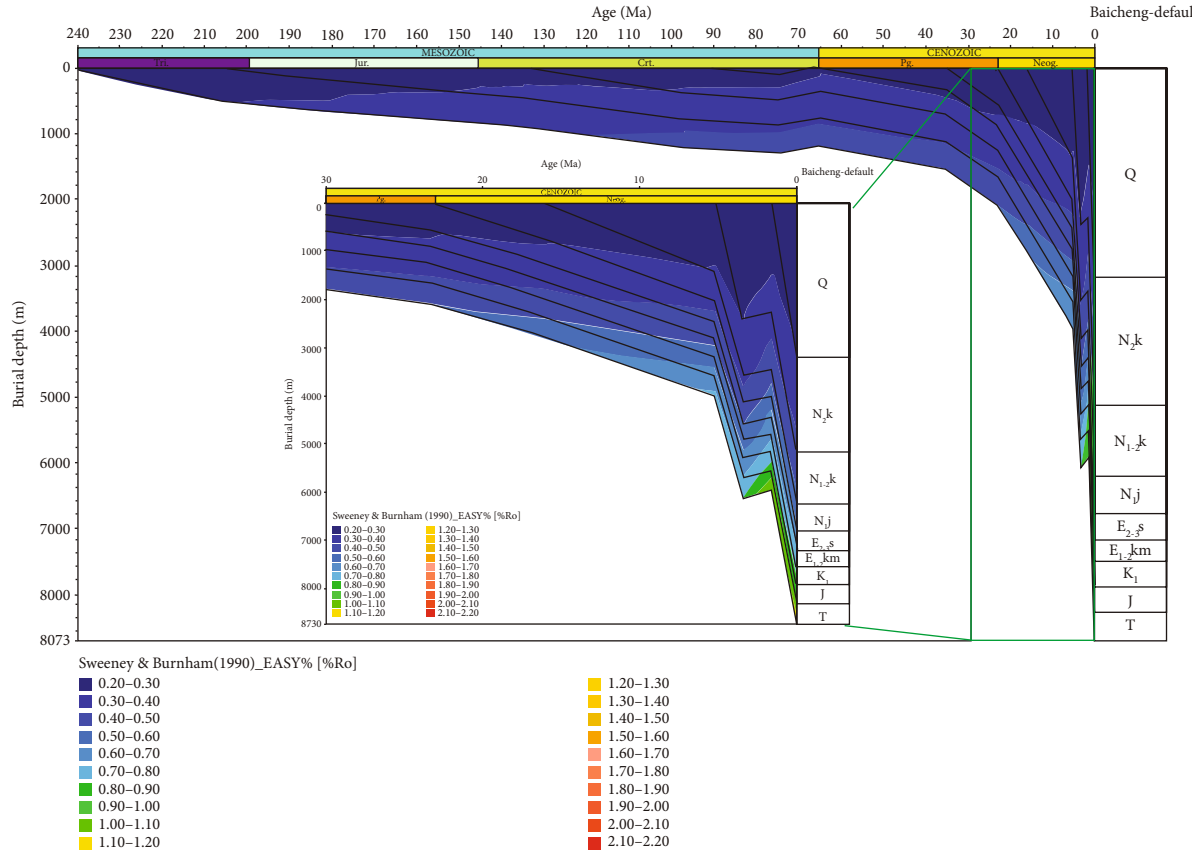

Figure 7: The burial and thermal history of the BC-1 well in the Baicheng Sag center.

stack since the $N_{1\text{-}2}k$ period caused the source rock to rapidly enter the high-over mature generation stage, quickly generating a lot of dry gas in the late stage. (4) On the south side of the Baicheng Sag, Xiqiu structural belt, and south slope belt, the sedimentation was always slow and steady. The source rock Ro increased slowly but was still at a lower mature stage, with a maximum Ro of 0.8–1.3%, still in the oil generation and wet gas generation stages.

Contrast of the source rock evolution sections that cut through the wells Keshen-2, Keshen-1, and Dabei-1 (Figure 9), which shows a similar regulation. First, from the northern monocline zone to the Kelasu structural belt, Baicheng Sag, and southern slope belt, the thermal maturity of source rocks initially increased and then decreased. They reached the maximum value in the deeper part of the Kelasu structural belt; that is, the maximum maturity center is located in the Kelasu thrust belt, rather than in the current Baicheng Sag center. Second, from the west to the east of the structural belt, the maximum source rock Ro was attained in the middle of the structural belt in the Keshen-5 and Keshen-1 well areas and decreased towards both sides. Third, on the time scale, source rocks near the Piedmont side of the thrust belt matured earlier, while the source rocks close to the depression matured much later.

4.3. Source Rock Maturity Distribution. Based on the measured Ro data and basin simulation results, the Ro contour map of the top Triassic in the Kuqa foreland basin was compiled (Figure 5). It can be seen that the mature hydrocarbon generation center in the Kuqa Basin is located in the deep part of the Kelasu-Dongqiu structural belt, rather in today's Baicheng and Yangxia Sag centers. Moreover, the maximum hydrocarbon mature center is located in the Keshen-2 and Keshen-5 well areas, with Ro values ranging between 2.4 and 3.0%, indicating that the source rock was already in the high-over mature gas generation stage. The spreading direction of the Ro contour is consistent with the strike of the Kuqa Basin, which extends in an east-west direction in a narrow and long band. The mature hydrocarbon generation center lies in the structural line along the Bozi-1, Dabei-3, Keshen-7, Dongqiu-8, and Dina-2 wells, and the source rock maturity is over 1.6%, reaching the high-over mature gas generation stage. The source rock maturity gradually reduced with distance from the mature center. The source rock in the northern piedmont belt and Wushi Sag, which mainly generated oil, had relatively lower maturity, ranging between 0.5 and 1.0% in the low mature to mature stage. The source rock maturity in the south slope belt and eastern part of Yangxia Sag ranged from 0.8 to 1.2% in the main oil generation stage.

Some previous researchers considered the mature center of the source rock to be located in the center of the Baicheng Sag and Yangxia Sag [10–12]. This is mainly because they did not consider the effect of rapid subsidence and a huge thick salt layer on the maturation of source rock but just predicted the source rock Ro in the deep sag center using the relationship of Ro with depth. Source rocks in Baicheng and Yangxia

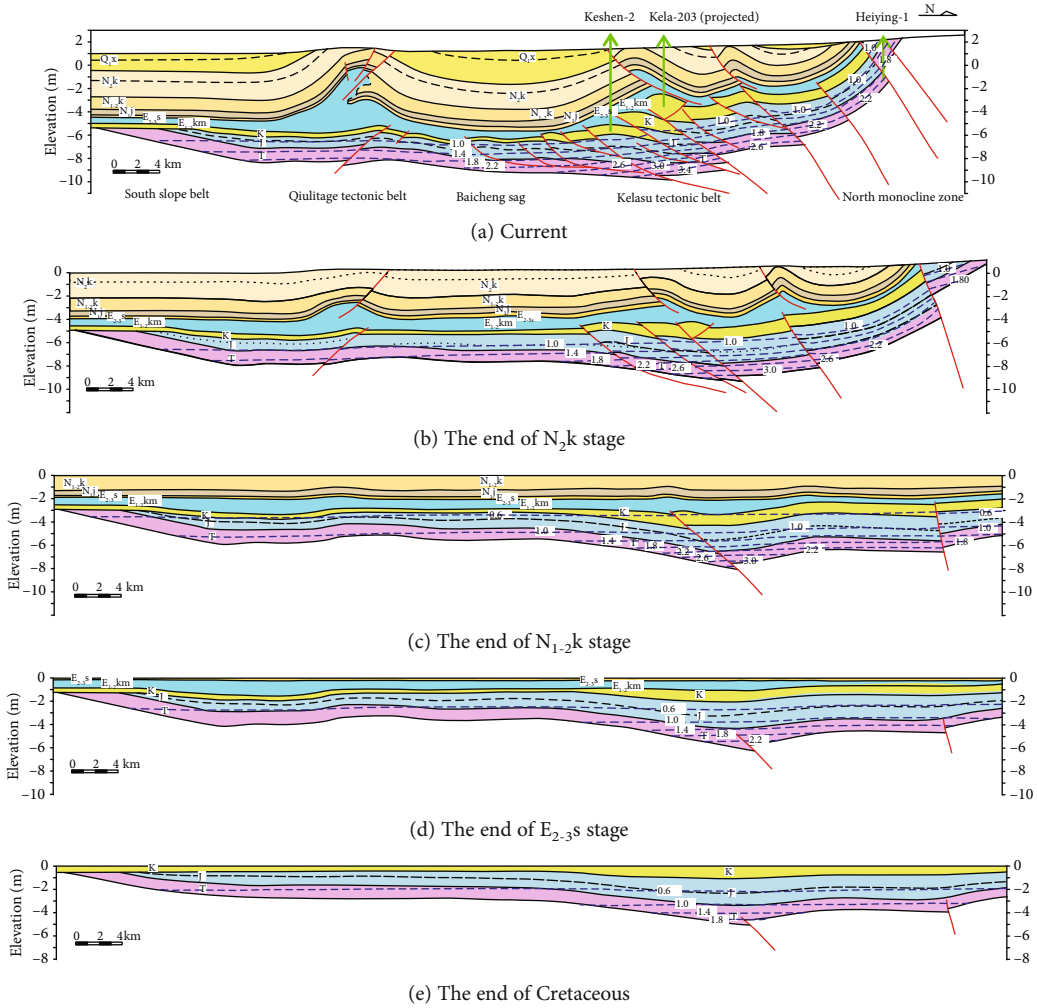

Figure 8: The structural and thermal evolution map of the geological section (the Keshen-2 well).

Sag have the largest current depth, thus making them conclude that source rocks in the Baicheng and Yangxia Sag may have the maximum Ro.

Previous studies have shown that differences in the nature of oil and gas phases are mainly controlled by the source rock maturity and accumulation processes, which are closely related to each other [14, 24, 27, 45]. Source rock evolution had a vital influence on the nature of oil and gas phases and maturity distribution in the Kuqa foreland basin. Hydrocarbon generation in the Triassic and Jurassic source rocks is characterized by dry gas in the inner zone, condensate gas in the middle zone, and oil in the outer zone (Figure 5; Table 3).

5. Discussions

5.1. The Effect of Overthrusting on Source Rock Maturity. The overthrusting stack effect in the foreland thrust belt often occurs in a short time, which causes a sudden increase or decrease in the thrust fault block depth, and its effect on source rock maturation cannot be ignored [7, 38, 46]. The overthrusting impact on the source rock Ro is mainly reflected in two cases. (1) In one case, the overthrusting occurred after source rock Ro stereotyping. This mainly occurs in the northern piedmont zone and north side of the thrust belt, and the thrust fault causes the original relationships of Ro and depth to become more complicated. Considering the Yixi-1 well as an example, it is located in the Yiqikeleke tectonic belt and has a complex thrust structure and many repeated strata. At a depth of 1741.5 m, a thrust fault occurs, which formed in the $N_{1\text{-}2}k$ stage. The source rock Ro was stereotyped before the fault occurrence, with the Ro of J_1y source rock at 0.9% and J_2kz at 0.75%. When a thrust fault occurs, the J_1y source rock is pushed up to 892 m in the hanging wall, and the footwall is a lower mature J_2kz source rock, thereby complicating the relationship between Ro and depth. (2) In another case, overthrusting occurred before the source rock Ro was stereotyped. This case occurs mainly in the leading edge of the thrust belt formed very late. The overthrusting caused a sudden increase in the footwall depth. When the stack thickness was very large, the Ro of the footwall source rock would increase significantly. Yang et al. [38] used an artificial well to simulate the impact of overthrusting on the source rock Ro. The overthrust fault formed after the $N_{1\text{-}2}k$ stage caused a stack stratum thickness of 2878 m. Before overthrusting, the J-T

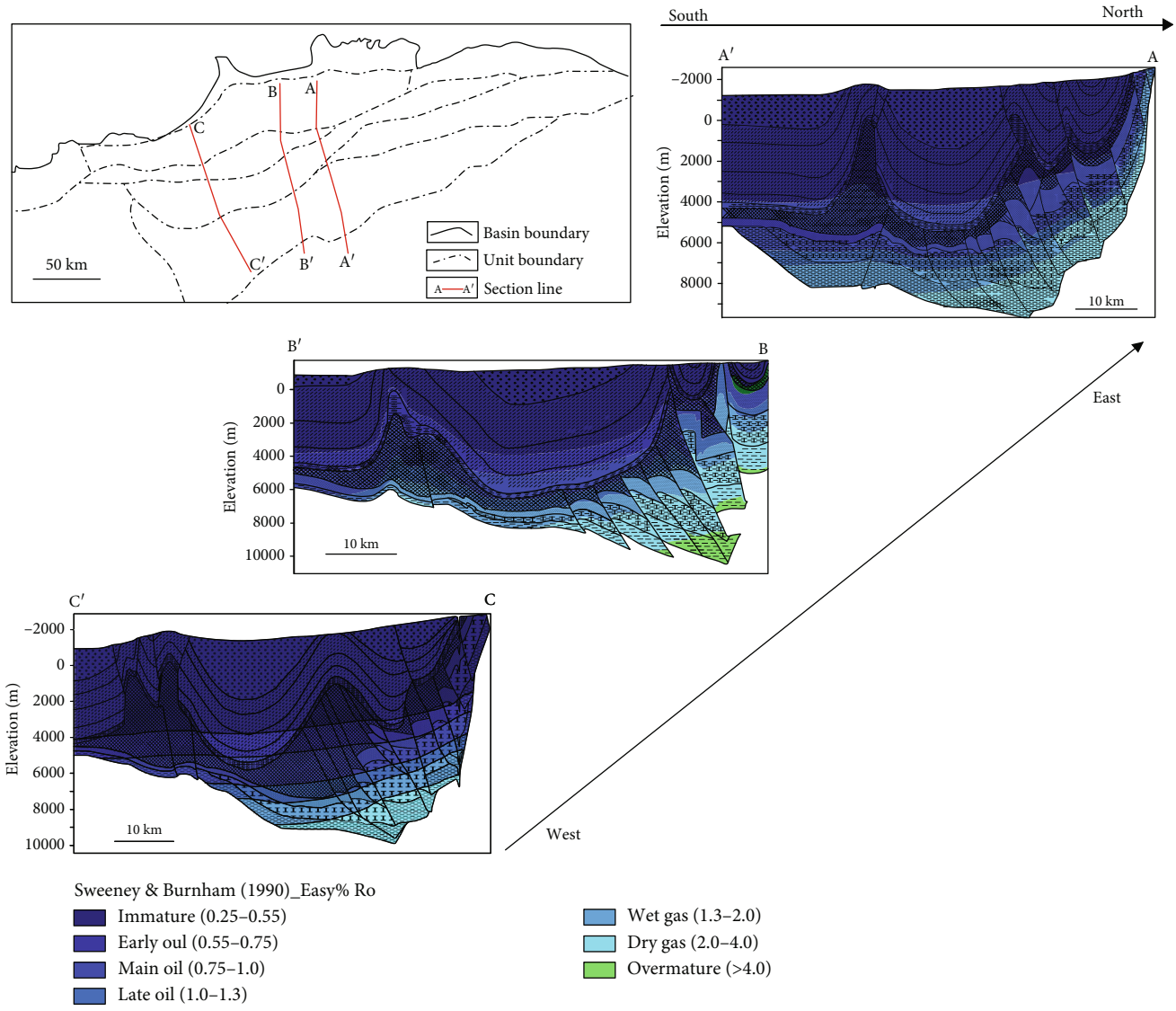

Figure 9: Contrast of thermal modeling results between three north-south geological profiles.

source rock Ro was lower than 0.8%. If we assume that there is no overthrusting, the late burial increases Ro by up to 1.6%. Considering the overthrusted stack thickness, the source rock Ro increased up to 3.4%; thus, the overthrusting created a difference in Ro larger than 1.8% (Figure 10). The dramatic increase in Ro in a short time indicated the impact of overthrusting on the source rock Ro.

5.2. The Effect of Salt Rock and Its Flow on the Source Rock Ro. Salt rock with high thermal conductivity facilitates the upward conduction of heat, causing the subsalt strata temperature to decrease. Thus, the large thick salt rock had a cooling effect on the overlying strata [38, 47]. This cooling effect is proportional to the thickness of the salt rock; the greater the thickness, the greater is the decrease in temperature. The salt rock thickness is up to 3000 m, with large lateral variations in the Kuqa foreland basin; thus, its effect on the heat flow and temperature must be considered.

A salt anticline or salt dome is formed because of the plastic flow of the salt layer in the local salt thickening area in the compressive stress environment of the Kuqa foreland basin, which constitutes the core of the Kelasu and Qiulitage tectonic belt [13, 48, 49]. The local thickening of salt layer caused thermal aggregation due to the difference of thermal conductivity between salt rock and other lithologies, forming the "hot chimney effect" [41], which decreases and increases the geothermal gradient and Ro in the subsalt layer and suprasalt layer, respectively. Figure 11 shows the current temperature simulation results of the geological profile through the Keshen-2 well. In places where the salt layer thickens, such as in Kelasu and the Xiqiulitage tectonic belts, the subsalt layer has a lower temperature at the same depth, and the surface heat flow is relatively large owing to the hot chimney effect. In Baicheng Sag, a higher temperature in the subsalt layer and lower surface heat flow are observed due to the decreased thickness of the salt layer.

Table 3: Hydrocarbon phases and methane carbon isotope data for different zones.

Zone	Source rock Ro (%)	Hydrocarbon phase	Typical reservoir	Phase type	Gas/oil ratio (m^3/m^3)	Gas drying coefficient	Methane carbon isotope (‰)
Inner zone	>2.0	Dry gas	Kela-2 gas field	Dry gas	114676	0.992~0.994	-28.24~ -26.16
			Keshen-2 gas reservoir	Dry gas	–	0.993~0.994	-28.3
			Keshen-5gas reservoir	Dry gas	–	0.997	-26.4
			Keshen-1gas reservoir	Dry gas	–	0.996	-27.88
Central zone	1.2-2.0	Condensate gas (low condensate oil content)	Dabei-1gas field	Condensate gas	38467	0.94~0.97	-31.9 ~ -29.73
			Dabei-3 gas field	Condensate gas	10757	0.985	-30.1
			Bozi-1 gas reservoir	Condensate gas	8517	0.86	-35.3
			Dina-2 gas reservoir	Condensate gas	12137	0.89~0.91	-33.2
			Dina-1gas field	Condensate gas	12476	0.89~0.91	-34.7 ~ -34.0
			Yina-2 gas reservoir	Condensate gas	8690	0.96	-34.8 ~ -32.2
Outer zone	0.6-1.2	Oil, volatile oil, condensate gas (high condensate oil content)	Shenmu-1oil reservoir	Oil	405	0.70~0.826	-35.4 ~ -35.8
			Yilake condensate gas	Condensate gas	1182	0.80~0.847	-35.99
			Quele-1 oil reservoir	Oil	342	0.81~0.85	-34.9
			Yangta-5 oil reservoir	Oil	647	0.79~ 0.84	-38.7 ~ -37.9
			Yingmaili oil field	Volatile oil	366~ 2796	0.91~ 0.93	-37.01~ -36.84
			Yaha gas field	Oil, volatile oil, condensate gas	225-1262	0.82-0.87	-38.74~ -33.4
			Tiergen gas field	Condensate gas	1677	0.82-0.84	-36.8 ~ -35.2

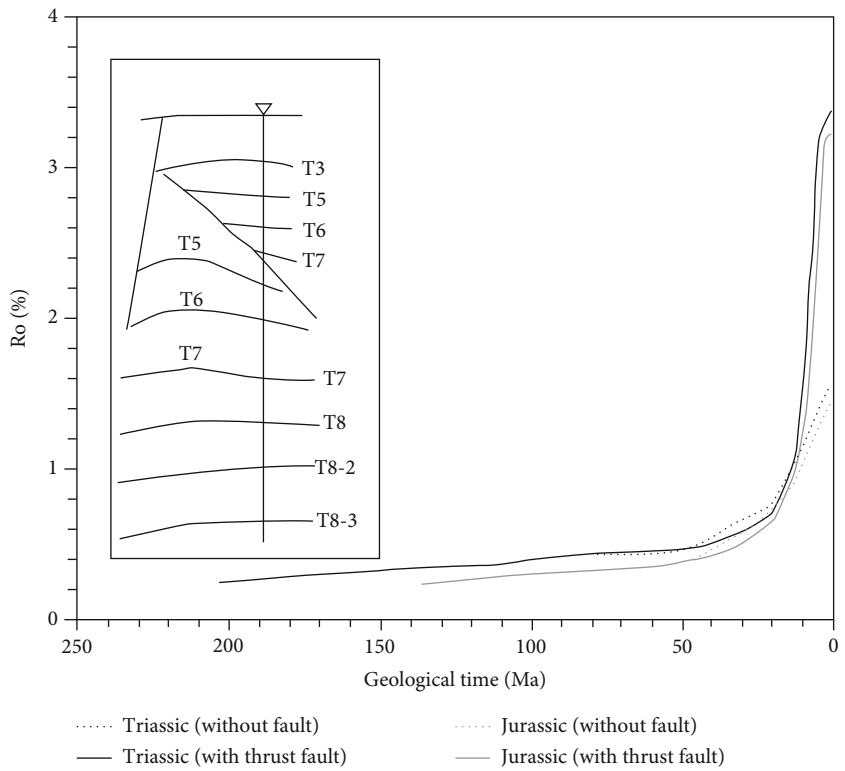

Figure 10: The effect of the thrust fault on the source rock maturity illustrated by a virtual well simulation.

5.3. The Control of Source Rock Maturity Evolution on Hydrocarbon Accumulation Process. A study on the hydrocarbon generation history showed that the large-scale oil generation began since the Neogene with two peaks in oil generation; whereas, gas generation mainly began since the Kuqa stage (Figure 12). The tectonic deformation in the Kuqa foreland basin began in the early Himalayan stage and stereotyped in the late Himalayan stage. Therefore, the strong tectonic movement in the Himalayan stage effectively matched various accumulation elements in a short period

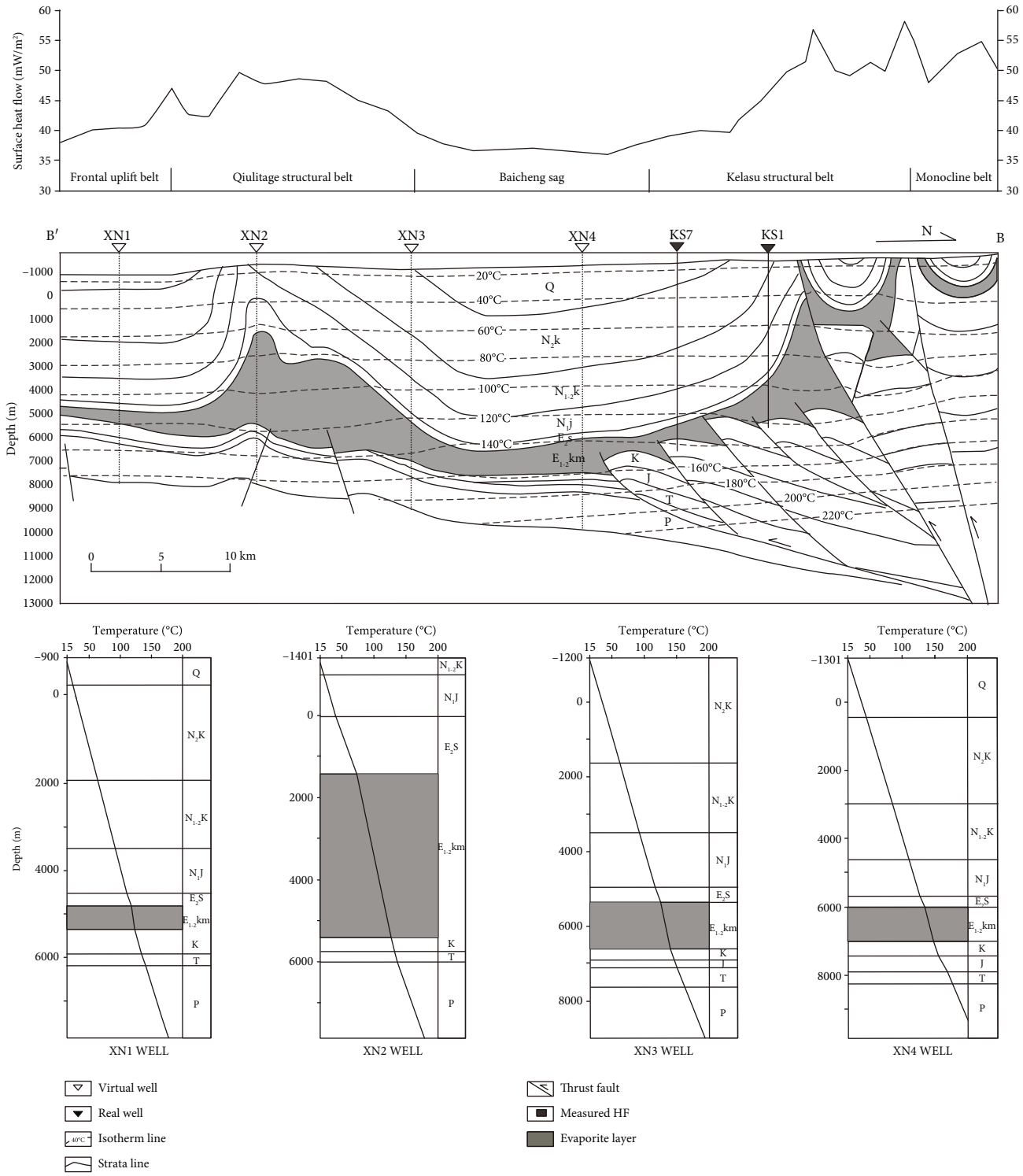

Figure 11: Temperature field in section B-B′ and the influence of evaporate rock on the temperature and HF distribution.

[50, 51]. In time, the trap formation time was in good agreement with the hydrocarbon generation and expulsion time, providing good conditions for oil and gas filling and accumulation. The matching of the multistage tectonic activity, hydrocarbon generation, and expulsion determines the characteristics of the multistage oil and accumulation, with late accumulation being dominant [13, 14, 25, 45]. Due to the rapid subsidence controlled by the strong compression in the Kuqa stage, the amount of gas generation increased rapidly from 5 Ma. The gas generation rate was up to 15–20 mg/gTOC/Ma, constituting highly efficient gas kitchens mainly distributed in the Kelasu and East Qiulitage tectonic belt (Figure 13). The distribution of highly efficient gas kitchens also determines the late gas mass accumulation

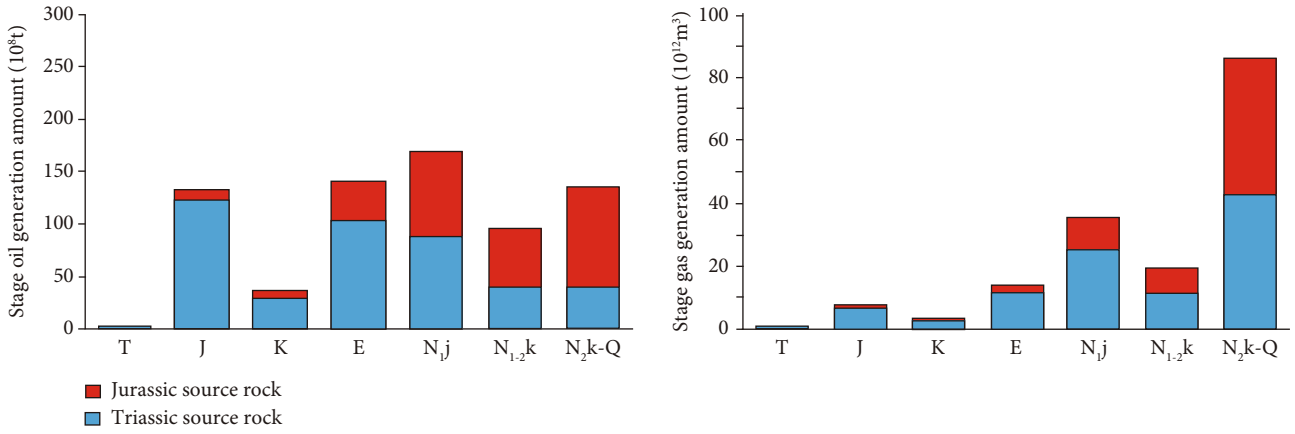

Figure 12: Hydrocarbon generation history of the J-T source rock in the Kuqa foreland basin.

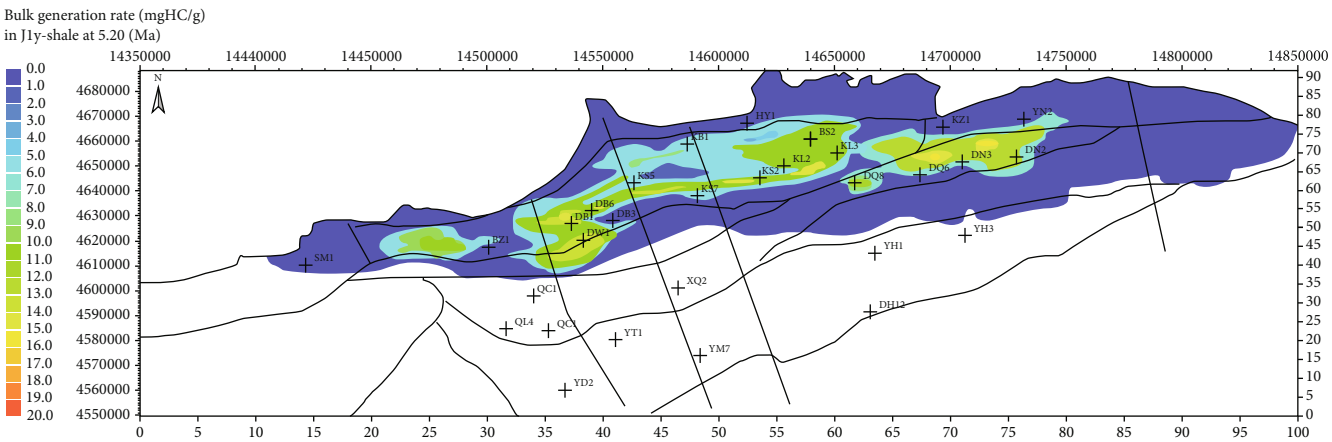

Figure 13: The bulk hydrocarbon generation rate of J_1y source rock (5.2 Ma).

area, which is consistent with the current discovery of large gas fields.

The spatial and temporal differences in the thermal and tectonic evolution of the Mesozoic source rock in the Kuqa foreland basin determine the significant difference of hydrocarbon accumulation processes in different structural zones (Figure 11). In the northern piedmont zone, source rocks had been in the mature stage since the N_1j-N_{1-2}k period, and oil was expelled and accumulated in the early formed structural traps. Subsequently, hydrocarbon generation stagnated with the late uplift and erosion, and the ancient oil reservoirs were destroyed; thus, the main reservoir types in the piedmont zone are residual oil reservoirs. In the Kelasu zone on the north side of the Kelasu structural belt, the source rock entered the mature stage during the N_{1-2}k period, and a large amount of oil was generated and accumulated into the early formed structural traps. However, the strong tectonic activity since the N_2k period destroyed these ancient oil reservoirs. Rapid subsidence causes source rocks to generate gas quickly in the late stage, and dry gas accumulates in the undestroyed traps under good preservation conditions, forming reservoirs containing dry gas with a small amount of residual crude oil, such as the Kela-2 gas field [25] and Dabei gas field [26]. In the Keshen zone on the north side of the Kelasu structural belt and north Baicheng area, source rocks had not yet reached the mature stage at the N_{1-2}k period. Rapid subsidence since the N_2k period resulted in rapid gas generation in the late stage, and the dry gas accumulated in the newly formed subsalt layer and extended southward into structural traps, forming dry gas reservoirs with late-generated dry gas, such as the Keshen-5 and Keshen-2 gas reservoirs. In the extensive area of the south slope zone, the source rock pinched out gradually southward, and the maturity of the neighboring source rocks was always low. Until the rapid subsidence in the N_2k period, the source rocks entered the mature stage. After their long-distance migration, hydrocarbons accumulated in favorable structural, lithological, and stratigraphic traps, thus forming oil and gas reservoirs in the late stage [18, 24]. The maturity of oil and gas here is relatively lower than that of the northern thrust belt. It is the time sequence of the thermal evolution of source rock and structural trap formation; their matching determines the different accumulation processes and oil and gas compositions in the different structural belts of the Kuqa foreland basin.

5.4. The Contribution of Stacked Source Rocks in the Thrust Belt to Hydrocarbon Generation. In the subsalt deep layer in the Kuqa foreland thrust belt, the J-T source rock was

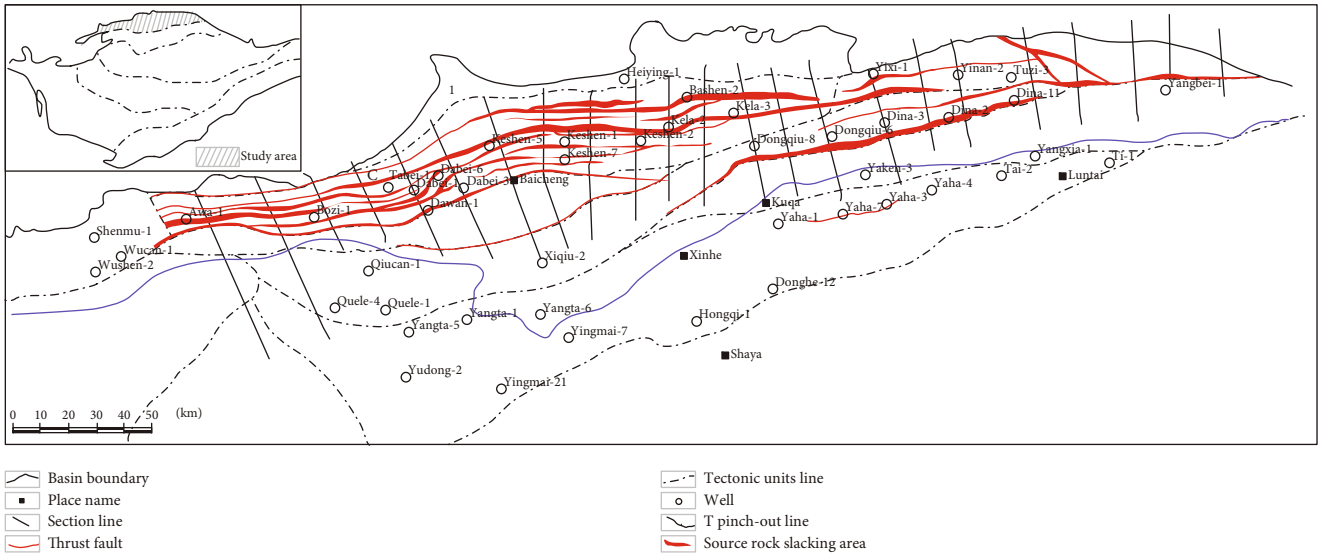

Figure 14: The source rock stacking areas related to the thrust faults in the Kuqa foreland basin.

vertically stacked, caused by multiple thrust faults. The mass vertical stacking of source rock makes the underlying source rock Ro increase, and the source rock thickness and hydrocarbon generation intensity per unit area also increase; thus, source rock generation centers are formed with super high generation intensity within a short distance. According to the latest interpreted structural map and 25 cross-sectional profiles, we calculated the stacking area of the source rock around 18 large-scale thrust faults, with a total area of 1585 km^2 (Figure 14). The source rock stacking areas are mainly distributed in the Kelasu tectonic belt. Hydrocarbon generation amount of the stacking source rocks can be calculated by multiplying the stacking area and average hydrocarbon generation intensity. The results show that the amount of gas generated from the stacking part of the source rock is 197.6×10^{12} m^3, accounting for 14.5% of the total gas generation. Moreover, the oil generation amount from the stacking part of the source rock is 55.9×10^8 t, accounting for 7.8% of the total oil generation. The vertical stacking of the source rock significantly increased the hydrocarbon generation intensity in the deep layer of the thrust belt, which is more favorable for large-scale oil and gas accumulation.

The effective stacking of source rock gas generation centers with high generation intensity and rate, a large number of zonally distributed and vertically stacked subsalt structural traps, good quality reservoir facies, and huge thick salt caprocks creates favorable geological conditions for gas enrichment in the Kelasu foreland thrust belt [49, 52]. This is the main reason for the discovery of many large gas fields such as Kela-2, Dabei, and Keshen-2 gas field, which form gas reserves greater than one trillion cubic meters in the Kelasu tectonic belt.

6. Conclusions

From the thermal modeling of the complex extrusional structural profiles in the thrust belt, a systematic recognition of the source rock maturity evolution, hydrocarbon generation, and accumulation characteristics in the Kuqa foreland basin has been conducted.

(1) In the north-south direction, from the piedmont zone, Kelasu tectonic belt, Baicheng Sag, and west Qiulitage tectonic belt to the southern slope belt, a large difference in the source rock thermal evolution history is observed. In the east-west direction, the source rock Ro is the largest in the Keshen-5 to Keshen-2 well areas in the middle of the Kelasu tectonic belt and decreases on both sides

(2) The sequences of the hydrocarbon generation and structural trap formation in time and space determine the different hydrocarbon accumulation processes and compositions in different structural belts

(3) Owing to the rapid subsidence controlled by the strong compression in the Kuqa stage, the amount of gas generation increased rapidly from 5 Ma, with a gas generation rate of up to 15–20 mg/gTOC/Ma; the distribution of the high-efficiency gas kitchen controlled the late gas accumulation and enrichment

(4) The effective stacking of the gas generation centers, subsalt structural traps, good quality reservoir facies, and huge thick salt caprocks creates favorable geological conditions for gas enrichment in the Kelasu foreland thrust belt. Thus, the subsalt deep layer in the Kelasu and East Qiulitage tectonic belts has a great resource and exploration potential and is still the main field for oil and gas exploration in the Kuqa foreland basin

Data Availability

Some or all data, models, or code generated or used during the study are available from the corresponding author by request.

Conflicts of Interest

The authors declare that they have no known competing financial interests or personal relationships that could have appeared to influence the work reported in this paper.

Authors' Contributions

Chengfu Lyu and Xixin Wang designed the experiment and performed the experiment. Xuesong Lu and Qianshan Zhou did the work of data processing and text editing. Ying Zhang and Zhaotong Sun drew and revised the figures in the paper. Liming Xiao and Xin Liu modified the language of the article in the process of revising the paper.

Acknowledgments

This research was financed by the China National Science Major Project (No. 2016ZX05003-002; 2016ZX05003-004) and PetroChina Science and Technology Project (No. 2019B-0506; 2019A-0210). We acknowledge the PetroChina Tarim Oilfield Company for their enthusiastic help and support by providing seismic profiles and drilling data.

References

[1] D. F. He and D. S. Li, *Tectonic Evolution and Petroleum Accumulation of Tarim Basin*, Geological Press, Beijing, 1996.

[2] C. Z. Jia, *The Features of Structure and Petroleum Geology in Tarim Basin of China*, Petroleum Industry Press, Beijing, 1997.

[3] C. Z. Jia, D. F. He, and Z. Y. Lei, *Petroleum Exploration in Foreland Thrust Belts*, Petroleum Industry Press, Beijing, 2000.

[4] Z. L. Kang and G. M. Zhai, "The foreland basins and hydrocarbon accumulations in China," *Acta Petrotia Sinica*, vol. 16, no. 4, pp. 1–8, 1995.

[5] H. F. Liu, H. S. Liang, L. G. Cai, X. Yiping, and L. Liqun, "Evolution and structural style of Tianshan and adjacent basins, north western China," *Geosciences*, vol. 19, no. 6, pp. 727–741, 1994.

[6] G. Y. Zhang, F. J. Chen, and X. W. Wang, "Deformation styles and distribution of the northern Tarim Basin," *Geosciences*, vol. 19, no. 6, pp. 755–768, 1994.

[7] D. Deming and D. S. Chapman, "Thermal histories and hydrocarbon generation: example from Utah-Wyoming thrust belt," *AAPG Bulletin*, vol. 73, no. 12, pp. 1455–1471, 1989.

[8] D. Deming, "Catastrophic release of heat and fluid flow in the continental crust," *Geology*, vol. 20, no. 1, pp. 83–86, 1992.

[9] W. A. Yonkee, W. T. Parry, R. L. Bruhn, and P. H. Cashman, "Thermal models of thrust faulting: constraints from fluid-inclusion observations, Willard thrust sheet, Idaho-Utah-Wyoming thrust belt," *Geological Society of America Bulletin*, vol. 101, no. 2, pp. 304–313, 1989.

[10] D. G. Liang, J. P. Chen, and B. M. Zhang, *The Generation of Continental Oil and Gas in Kuqa Depression*, Petroleum industry press, Beijing, 2004.

[11] F. Y. Wang, S. C. Zhang, B. M. Zhang, and M. J. Zhao, "Organic maturity of Mesozoic source rocks in Kuqa depression, Tarim basin," *Xinjiang Petroleum Geology*, vol. 20, pp. 221–224, 1999.

[12] F. Y. Wang, Z. L. Du, Q. Li et al., "Organic maturity and hydrocarbon generation history of the Mesozoic oil-prone source rocks in Kuqa depression, Tarim Basin," *Geochimica*, vol. 34, pp. 136–146, 2005.

[13] Z. M. Wang and H. S. Long, "Different hydrocarbon accumulation histories in the Kelasu-Yiqikelike structural belt of the Kuqa foreland basin," *Acta Geologica Sinica: English Edition*, vol. 84, pp. 1195–1208, 2010.

[14] M. J. Zhao, Y. Song, and S. F. Qin, "The multi-stage formation of oil-gas pools and late-stage accumulation of gas in the foreland basins in central and western China," *Earth Science Frontiers*, vol. 12, no. 4, pp. 525–533, 2005.

[15] S. Q. Li, X. Wang, and J. Suppe, "Compressional salt tectonics and synkinematic strata of the western Kuqa foreland basin, southern Tian Shan, China," *Basin Research*, vol. 24, no. 4, pp. 475–497, 2012.

[16] X. Wang, Z. M. Wang, H. W. Xie et al., "Cenozoic salt tectonics and physical models in the Kuqa depression of Tarim Basin, China," *Scientia Sinica Terrae*, vol. 40, pp. 1655–1668, 2010.

[17] Z. L. Du, F. Y. Wang, S. C. Zhang, B. M. Zhang, and D. G. Liang, "Gas generation history of Mesozoic hydrocarbon kitchen in Kuqa depression, Tarim basin," *Geochimica*, vol. 35, pp. 419–431, 2006.

[18] J. Z. Zhao and J. X. Dai, "Accumulation timing and history of Kuqa petroleum system, Tarim basin," *Acta Sedimentologica Sinica*, vol. 20, no. 2, pp. 314–318, 2002.

[19] X. X. Zhou, "The characteristics of tertiary gypsum caprock and its impact on the oil-gas accumulation in the Kuqa depression," *Journal of Palaeogeopraphy*, vol. 2, pp. 51–57, 2000.

[20] S. Chen, L. Tang, Z. Jin, C. Jia, and X. Pi, "Thrust and fold tectonics and the role of evaporites in deformation in the Western Kuqa Foreland of Tarim Basin, Northwest China," *Marine and Petroleum Geology*, vol. 21, no. 8, pp. 1027–1042, 2004.

[21] L. J. Tang, C. Z. Jia, Z. J. Jin, S. P. Chen, X. J. Pi, and H. W. Xie, "Salt tectonic evolution and hydrocarbon accumulation of Kuqa foreland fold belt, Tarim Basin, NW China," *Journal of Petroleum Science & Engineering*, vol. 41, no. 1-3, pp. 97–108, 2004.

[22] L. J. Tang, C. Z. Jia, X. J. Pi, S. Chen, Z. Wang, and H. Xie, "The salt-related structural styles in Kuqa foreland fold belt," *Science in China (D)*, vol. 33, pp. 38–46, 2004.

[23] Z. P. Xu, Y. Li, Y. J. Ma, W. Chao, Y. Xianzhang, and L. Qing, "Future gas exploration orientation based on a new scheme for the division of structure units in the central Kuqa depression, Tarim Basin," *Natural Gas Industry*, vol. 3, pp. 31–36, 2011.

[24] X. X. Zhou, "Phase state of oil & gas pools in Kuqa petroleum system," *Natural Gas Industry*, vol. 21, pp. 82–85, 2001.

[25] X. S. Lu, K. Y. Liu, Q. G. Zhuo, M. Zhao, S. Liu, and S. Fang, "Palaeo-fluid evidence of the multi-stage hydrocarbon charges in Kela-2 gas field, Kuqa foreland basin, Tarim Basin," *Petroleum Exploration and Development*, vol. 39, no. 5, pp. 574–582, 2012.

[26] S. Zhang, B. Zhang, G. Zhu, H. Wang, and Z. Li, "Geochemical evidence for coal-derived hydrocarbons and their charge history in the Dabei Gas Field, Kuqa thrust belt, Tarim Basin, NW China," *Marine and Petroleum Geology*, vol. 28, no. 7, pp. 1364–1375, 2011.

[27] C. Ling, Z. Guangyou, Z. Bin, W. Zhigang, and W. Yonggang, "Control factors and diversities of phase state of oil and gas pools in the Kuqa petroleum system," *Acta Geologica Sinica - English Edition*, vol. 86, no. 2, pp. 484–496, 2012.

[28] X. X. Wang, Y. M. Liu, J. G. Hou et al., "The relationship between synsedimentary fault activity and reservoir quality -

a case study of the Ek1 formation in the Wang Guantun area, China," *Interpretation*, vol. 8, no. 3, pp. sm15–sm24, 2020.

[29] G. L. Sheng, Y. L. Su, and W. D. Wang, "A new fractal approach for describing induced-fracture porosity/permeability/compressibility in stimulated unconventional reservoirs," *Journal of Petroleum Science and Engineering*, vol. 179, pp. 855–866, 2019.

[30] G. L. Sheng, H. Zhao, Y. L. Su et al., "An analytical model to couple gas storage and transport capacity in organic matter with noncircular pores," *Fuel*, vol. 268, p. 117288, 2020.

[31] B. P. Tissot, R. Pelet, and P. Ungerer, "Thermal history of sedimentary basins, maturation indices, and kinetics of oil and gas generation," *AAPG Bulletin*, vol. 71, pp. 1445–1466, 1987.

[32] P. Ungerer, J. Burrus, B. Doligez, P. Y. CHENET, and F. BESSIS, "Basin evaluation by integrated two-dimensional modeling of heat transfer, fluid flow, hydrocarbon generation, and migration," *AAPG Bulletin*, vol. 74, pp. 309–335, 1990.

[33] D. H. Welte and M. N. Yalcin, "Basin modelling—a new comprehensive method in petroleum geology," *Organic Geochemistry*, vol. 13, no. 1-3, pp. 141–151, 1988.

[34] T. Hantschel and A. I. Kauerauf, *Fundamentals of Basin and Petroleum Systems Modeling*, Springer, 2009.

[35] N. S. Qiu, "Thermal evaluation and hydrocarbon generation history of the sedimentary basins in western China," *Petroleum Exploration and Development*, vol. 29, pp. 6–8, 2002.

[36] L. S. Wang, C. Li, S. W. Liu et al., "Terrestrial heat flow distribution in Kuqa foreland basin, Tarim, NW China," *Petroleum Exploration and Development*, vol. 32, pp. 79–84, 2005.

[37] X. X. Wang, J. G. Hou, S. H. Li et al., "Insight into the nanoscale pore structure of organic-rich shales in the Bakken Formation, USA," *Journal of Petroleum Science and Engineering*, vol. 191, p. 107182, 2020.

[38] S. C. Yang, Q. Z. Lu, C. Z. Song, Y. S. Yuan, H. J. Wang, and S. B. Hu, "Evolution of Mesozoic source rock's organic maturation in Kuqa foreland basin and its influence factors," *Oil & Gas Geology*, vol. 26, pp. 770–777, 2005.

[39] G. Juergen, H. Ralph, and F. S. Reinhard, "Evaluation of hydrocarbon generation and migration in the Molasse fold and thrust belt (Central Earsten Alps, Austria) using structural and thermal basin models," *AAPG Bulletin*, vol. 98, no. 2, pp. 253–277, 2014.

[40] X. Wang, J. Hou, S. Song et al., "Combining pressure-controlled porosimetry and rate-controlled porosimetry to investigate the fractal characteristics of full-range pores in tight oil reservoirs," *Journal of Petroleum Science and Engineering*, vol. 171, pp. 353–361, 2018.

[41] F. Magri, R. Littke, S. Rondon, and J. L. Urai, "Temperature fields, petroleum maturation and fluid flow in the vicinity of salt domes," in *Dynamics of Complex Intracontinental Basins: the Central European Basin System*, R. Littke, U. Bayer, D. Gajewski, and S. Nelskamp, Eds., pp. 323–344, Springer, 2008.

[42] K. E. Peters and M. R. Cassa, *Applied Source Rock Geochemistry: Chapter 5: Part II. Essential Elements*, 1994.

[43] J. M. Hunt, *Petroleum Geochemistry and Geology*, W. H. Freeman and Company, New York, second edition, 1996.

[44] M. H. Hakimi, A. Ahmed, A. Y. Kahal, O. S. Hersi, H. J. Al Faifi, and S. Qaysi, "Organic geochemistry and basin modeling of Late Cretaceous Harshiyat Formation in the onshore and offshore basins in Yemen: Implications for effective source rock potential and hydrocarbon generation," *Marine and Petroleum Geology*, vol. 122, p. 104701, 2020.

[45] M. J. Zhao, Z. M. Wang, S. C. Zhang et al., "Accumulation and features of natural gas in the Kuqa foreland basin," *Acta Geologica Sinica*, vol. 79, pp. 414–422, 2005.

[46] J. D. Edman and R. C. Surdam, "Influence of overthrusting on maturation of hydrocarbon in Phosphoria Formation, Wyoming-Idaho-Utah overthrust belt," *AAPG Bulletin*, vol. 68, pp. 1803–1817, 1984.

[47] X. Z. Yang, G. L. Lei, G. W. Zhang, and D. Y. Zhao, "Effect of gypsum-salt rocks on hydrocarbon accumulation in Kelasu structural belt of Kuqa depression," *Xinjiang Petroleum Geology*, vol. 30, pp. 201–204, 2009.

[48] J. F. Qi, G. L. Lei, M. G. Li, and G. Yongxing, "Analysis of structure model and formation mechanism of Kelasu structure zone, Kuqa depression," *Geotectonica ET Metallogenia*, vol. 33, pp. 49–56, 2009.

[49] Z. M. Wang, "Formation mechanism and enrichment regularities of Kelasu subsalt deep large gas field in Kuqa depression," *Tarim Basin. Natural Gas Geoscience*, vol. 25, pp. 153–166, 2014.

[50] Z. X. Jiang, L. X. Li, Y. Song et al., "Control of neotectonic movement on hydrocarbon accumulation in the Kuqa foreland basin, west China," *Petroleum Science*, vol. 7, no. 1, pp. 49–58, 2010.

[51] Y. Song and X. S. Wang, "The controlling action of modern structural movement on the late accumulation of natural gas," *Natural Gas Geoscience*, vol. 14, pp. 103–106, 2003.

[52] J. H. Du, Z. M. Wang, S. Y. Hu, W. Qinghua, and X. Huiwen, "Formation and geological characteristics of deep giant gas provinces in the Kuqa foreland thrust belt, Tarim Basin, NW China," *Petroleum Exploration and Development*, vol. 39, no. 4, pp. 385–393, 2012.